Nomarski differential interference-contrast microscopy

by Walter Lang

II. Formation of the interference image

Part I of the general description of Nomarski differential interference-contrast microscopy dealt with the fundamentals and experimental designs of ZEISS interference-contrast equipment (12). This second part of the description will be devoted to the formation of the differential interference-contrast image (in the following called DIC image, following a suggestion by J. Gahm). For this purpose, the wavefronts of the Wollaston prism will be described first in Section 1. The background image, which depends on the differences of path length and amplitude of the interfering waves, is discussed in Section 2. The formation of the DIC image (Section 3) is explained with the aid of model objects. A detailed discussion of objects from the different fields of application of Nomarski DIC microscopy would be beyond the scope of this series of papers; it is therefore reserved for separate publication.

1. The wavefronts in the Wollaston prism

A wavefront is the line joining the points of identical phase within a wave packet (see, e. g., 1, 6, 11, 13, 14, 15, 23). The behavior of wavefronts in a Wollaston prism (18) will be explained with the aid of example a) of Fig. 1. In the lower crystal, a linearly polarized wave with the plane wavefront Σ is split into two plane-polarized components, viz. the ordinary wave and the extraordinary wave. Both waves have different refractive indices: with yellow sodium light of wavelength 589.3 mμ, the ordinary wave in a quartz crystal has a refractive index of n_o = 1.5442, the extraordinary wave one of n_{eo} = 1.5534. Consequently, the difference in refractive index is 0.0092, in other words, n_{eo} is almost 0.6 % larger than n_o. Since the propagation speed of the wave in the crystal is inversely proportional to the refractive index, it follows that the ordinary wave has a higher speed than the extraordinary wave [1]. As a result, the wavefront Σ_o is in advance of the wavefront Σ_{eo} in the lower prism.

So-called angular wave splitting occurs at the cemented surface, i. e. the ordinary and the extraordinary wave take different courses. The angle subtended by them is less than half a minute. In addition, the ordinary wave of the lower prism becomes the extraordinary wave in the upper prism, while the extraordinary wave of the lower prism becomes the ordinary wave in the upper prism (12, 15, 21). In case a) this means that in the upper prism the wavefront Σ_{eo} is in advance of the wavefront Σ_o because as Σ_o, Σ_{eo} has advanced beyond the second wave in the lower prism to such an extent that this advance is only slowly made up for in the upper prism. Since the angular splitting at the cemented surface is only very small, the geometrical paths of the two components in the central position of the Wollaston prism shown in the diagram are only slightly larger than in the lower half of the prism. Consequently, as the two waves emerge from the Wollaston prism, they have covered identical optical path lengths[2], i. e. both wavefronts leave the Wollaston prism simultaneously with zero path difference[2]. If after emerging from the Wollaston prism the two waves pass through air, the same refractive index applies to both of them, i. e. their speed is identical. As a result, the path difference between the two waves is maintained. In the special case a) it is zero.

If, for reasons that will be discussed later, a path difference is desired, this can be obtained by shifting the Wollaston prism perpendicular to the direction of the incident bundle of light. In case b), the advance of Σ_o over Σ_{eo} in the lower prism is such that it is compensated only partly in the upper half of the prism (wavefronts not shown): outside the Wollaston prism, Σ_{eo} advances in relation to Σ_o. The opposite case is shown in the example c).

In the experimental design of DIC equipment for transmitted light using two Wollaston prisms, a path difference can be introduced by shifting one of them because for the final DIC image it is of no importance whether the optical path difference is caused by the auxiliary prism in the condenser or whether it is introduced by means of the principal prism (12, 16, 17, 18, 20) located between objective and image. A displacement of the principal prism is given preference only for reasons of convenience. The most favorable conditions for this case follow from Fig. 1 if the diagram is imagined inverted. – If Nomarski prisms were utilized instead of Wollaston prisms, no basically new considerations would result with regard to the behavior of the wavefronts in the crystal (see 7, 18). The diagram thus obtained would merely be less clear than in the case of the Wollaston prisms discussed above.

2. The interference background image

In the following, the formation and interpretation of the *background* image in Nomarski DIC microscopy will be explained. By background image we understand the image of an object-free area in the specimen. With the ZEISS DIC equipment (and using white light for illumination of the object), this background can be made to appear black-and-white or gray or colored. This means that a multitude of different color phenomena may be encountered even if there is no microscopic object in the light path. These phenomena must not be attributed to a microscopic object, but considered as instrument characteristics, as equipment parameters[3]. A detailed explanation of the formation of the background image on one hand shows the multitude of optical staining possibilities. On the other hand it is intended to warn against possible sources of error in the interpretation of the interference image due to careless use of the equipment. – Before elaborating on the most essential characteristics of this equipment, a few concepts from the field of interference colors should be briefly reviewed.

Fig. 2 shows schematically the conditions in the case of the superposition of two

[1] This holds generally for positively uniaxial crystals such as quartz. The opposite applies to negatively uniaxial crystals such as calcite (1, 21).

[2] Optical path length (2, 11, 13, 14, 15, 24): Δ = nd, where n = refractive index, d = geometrical path. This is also called the path difference Γ, where Γ is preferably used for optical path differences, e. g. $\Delta_1 - \Delta_2$.

[3] In principle, these equipment parameters also apply to interference microscopes of other design, such as the Jamin-Lebedeff interference-contrast equipment made by ZEISS.

Fig. 1: Wavefronts in a Wollaston prism. For greater clarity, the angular wave splitting at the cemented surface and the distance between the wavefronts Σ_o and Σ_{eo} are exaggerated.

Richtung der optischen Achse des Kristalls = Direction of optic axis of crystal; parallel = parallel; senkrecht zur Zeichenebene = perpendicular to plane of diagram; Schwingungsebene des Lichtes = Vibration plane of light; unter 45° geneigt = inclined 45°; senkrecht = perpendicular; parallel zur Zeichenebene = parallel to plane of diagram; Wellenfronten = Wavefronts; der einfallenden Welle = of incident wave; der ordentlichen Welle = of ordinary wave; der außerordentlichen Welle = of extraordinary wave.

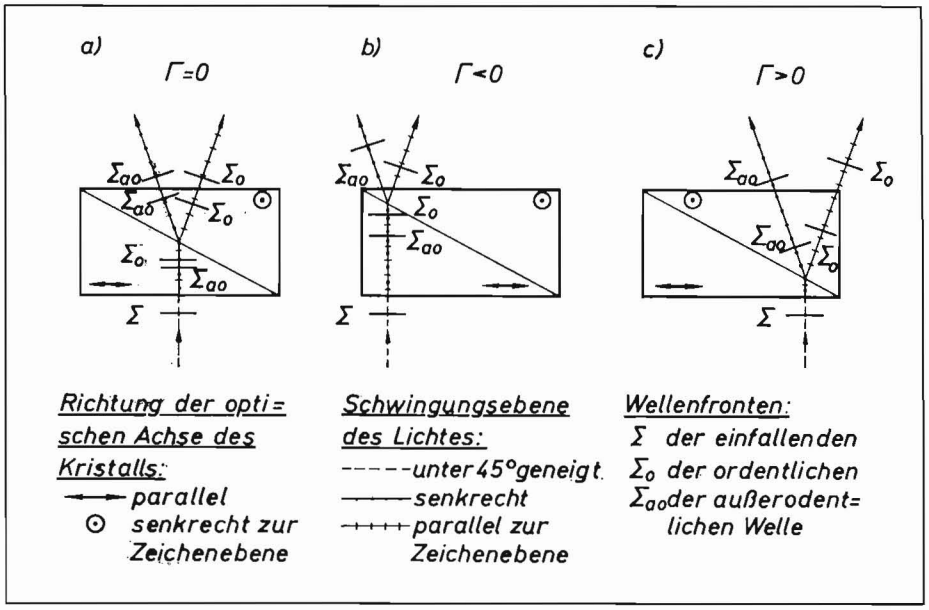

1

Fig. 2: Interference of white light. For simplification, only the colors blue, green and red are shown.

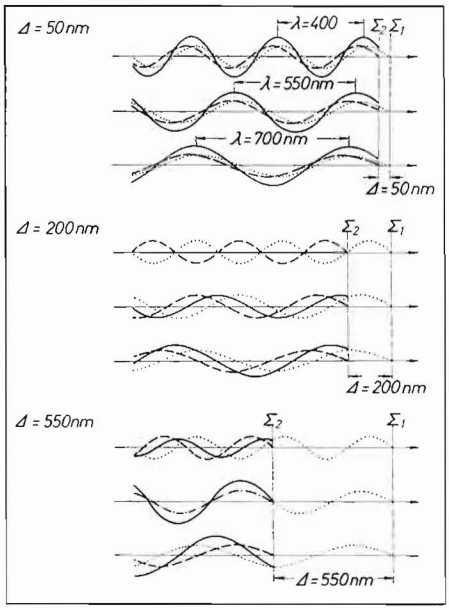

2

coherent wave packets of white light (11, 15, 22) with optical path differences Δ of 50, 200 and 550 mμ. For greater clarity, only three colors of the white light are shown, namely blue (wavelength λ = 400 mμ), green (λ = 550 mμ) and red (λ = 700 mμ). Making allowance for the sign, the interfering components (dotted and dashed curves) yield the solid curves as resulting waves. If the optical path difference between Σ_1 and Σ_2 is small, e. g. 50 mμ, as is shown in the upper part of the figure, then with all three colors the final curves have larger amplitudes than the individual curves: we then speak of constructive interference. The extreme is encountered if Δ = 0 or a whole multiple of the light wavelength. Thus in the lower part of the figure, the optical path difference of 550 mμ is equivalent to the wavelength of the green light. In this case the two components are "in phase", whereas, if Δ = 200 mμ, the two component beams of the blue light are of "opposite phase". They interfere destructively. This means that the white light is deprived of the blue component. The other final curves, in our example the green and red ones, will then mix uniformly in accordance with their intensity ratio[4] to form a so-called interference color. (To avoid misunderstandings, it should be pointed out already here that this interference color is not identical with that of the DIC image.)

Since the intensity ratio of the different colors varies with optical path difference, every path difference is associated with a characteristic interference color. However, this applies only to path differences which do not exceed the coherence length (see 11).

In Fig. 2 it was tacitly assumed that the superimposed components (dotted and dashed curves) vibrate in one and the same plane. With interference microscopes this precondition, which is indispensable for the interference of two coherent waves, is not given from the start, but must be brought about with the aid of an analyzer. The same holds for the Nomarski DIC equipment: as is evident from Fig. 3a), an analyzer arranged between the principal prism and the eyepiece (18) intercepts the waves with the vectors of electrical field strength $\vec{e}_1$ and $\vec{e}_2$ and allows only the components $\vec{e}_{1A}$ or $\vec{e}_{2A}$ coinciding with the vibration direction of the analyzer A to pass (see 1, 6, 7, 12). The components $\vec{e}_{1P}$ or $\vec{e}_{2P}$, however, which together give $\vec{e}_P$, are perpendicular to the transmission direction of the analyzer and therefore have no effect on the final DIC image. In addition, the components parallel to the transmission direction of the analyzer shown in Fig. 3a) are of opposite, but identical magnitude so that they cancel out. Transferring these results to ZEISS DIC equipment, Fig. 3a) corresponds to zero path difference, i. e. the field of view is dark. The Michel-Lévy color chart (19) reveals that zero path difference is equivalent to the interference color black.

If there is a path difference between the two waves emerging from the principal prism, then $\vec{e}_1$ and $\vec{e}_2$ differ in length (Fig. 3b). Consequently, the length of the components $\vec{e}_{1A}$ and $\vec{e}_{2A}$ also differs. In the DIC image,

[4] Due to the difference in wavelength the final curves of the different colors cannot interfere. The intensity ratio is therefore decisive for the resultant interference color.

Fig. 3: The effect of the analyzer in ZEISS DIC equipment. P = transmission direction of polarizer, A = transmission direction of analyzer, A′ = direction perpendicular to A, $\vec{e}$ = vector of electrical field strength, index 1 or 2 = waves emerging from principal prisms with mutually perpendicular vibration planes. a) crossed P and A. $\Gamma = 0$ between waves 1 and 2; b) same as a), but $\Gamma = 0$; c) P and A not rigorously crossed. $\Gamma = 0$; d) same as c), but $\Gamma = 0$.

Fig. 4: Wavefronts at different points in the light path and intensity distribution in the intermediate image plane of a DIC unit in accordance wih the diagram in the lefthand portion of the illustration. Cases A to D are distinguished by the path differences between the wavefronts Σ_1 and Σ_2.
Zwischenbildebene = Intermediate image plane; Analysator (135°) = Analyzer (135°); Hauptprisma = Principal prism; Objektiv = Objective; (Modell-) Objekt = (Model-) object; Kondensor = Condenser; Hilfsprisma = Auxiliary prism; Polarisator (45°) = Polarizer (45°); Fall = Case.

3

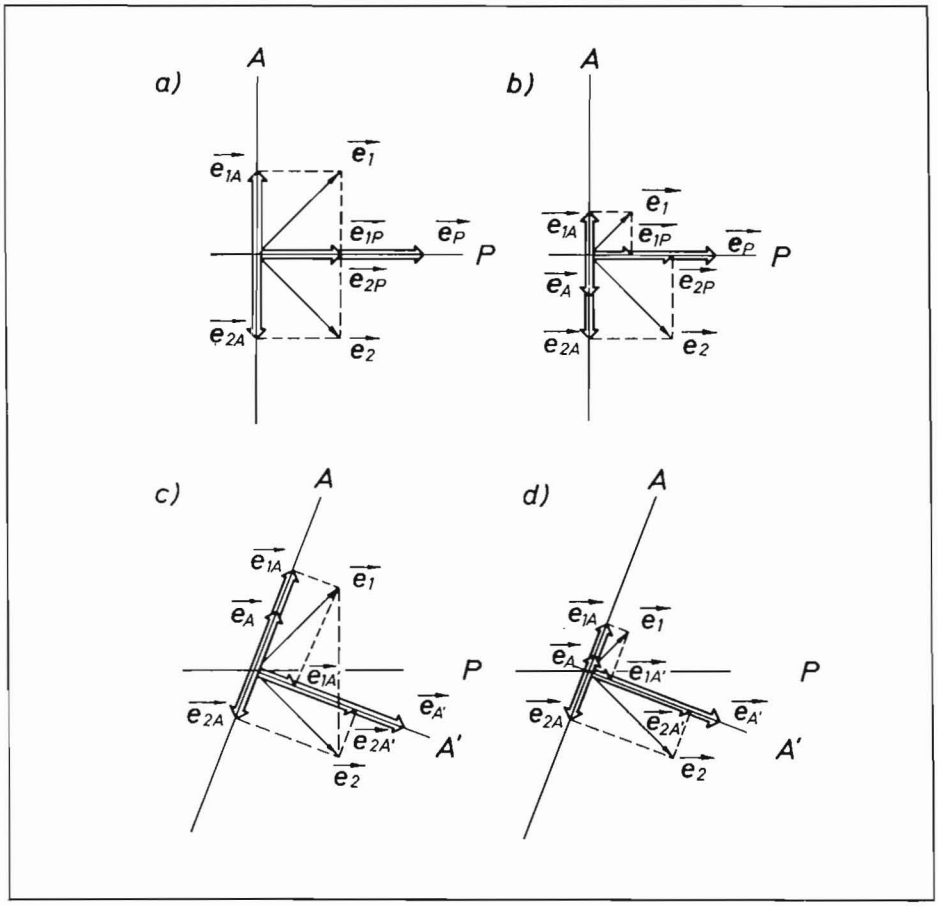

4

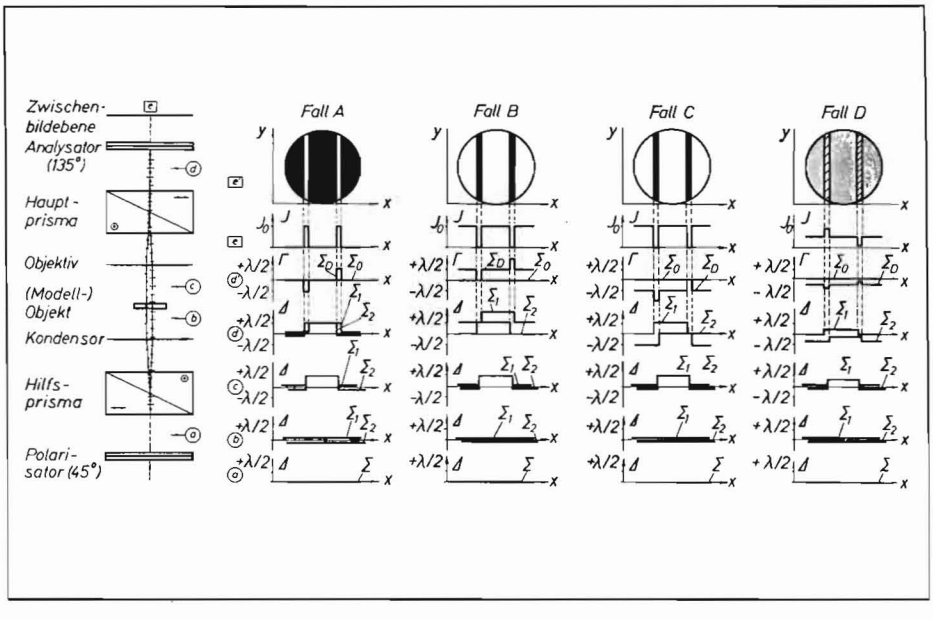

the resultant of these two vectors, namely $\vec{e}_A$, becomes effective. (The vector $\vec{e}_P$ resulting from $\vec{e}_{1P}$ and $\vec{e}_{2P}$ is perpendicular to the transmission direction of the analyzer and thus does not contribute to the DIC image.) – If the path difference is 50 mμ, e. g. as in Fig. 2, top, the DIC image will assume a hue between iron and lavender gray, as is also evident from the Michel-Lévy color chart (6). A gray blue to gray or deep red hue in the DIC image corresponds to a path difference of 200 or 500 mμ, respectively (see Fig. 2).

If polarizer and analyzer are not accurately crossed (Figs. 3c and d), the DIC image will be affected in a different way. While $\vec{e}_1$ and $\vec{e}_2$ are of identical length in Fig. 3c) (which corresponds to zero path difference), their components in the transmission direction of the analyzer, $\vec{e}_{1A}$ and $\vec{e}_{2A}$, are of different magnitude. The resultant $\vec{e}_A$ therefore differs from zero (in spite of zero path difference). It lights the image background. The vector $\vec{e}_A$ resulting from $\vec{e}_{1A}$ and $\vec{e}_{2A}$ is perpendicular to A and therefore cannot affect the interference image.

If, in addition, there is a path difference between the components 1 and 2, $\vec{e}_1$, $\vec{e}_2$ and thus $\vec{e}_{1A}$, $\vec{e}_{2A}$ will also differ in length (Fig. 3d). The resultant $\vec{e}_A$ strikes the DIC image in a different way than is the case in Fig. 3b). To avoid unnecessary difficulties in the interpretation of the DIC image, it is therefore advisable to work with crossed polarizer and analyzer.

3. The DIC image

In interference microscopes, the "object structure" seen in the microscopic image is the optical expression of very different physical magnitudes of the microscopic object. With the Nomarski DIC equipment described in this paper, the interference image of an isotropic phase object depends a) on the magnitude of the angular or lateral wave splitting and b) on the path difference between the two components (see also 6, 7, 11, 23). The path difference caused by a *transparent* object is given by the product of the refractive index and

geometrical thickness of the object. As is shown in Section 2, an additional path difference can be superimposed by means of the principal prism.

The path difference caused by an *opaque* object depends on the geometrical profile of the object and the phase retardation resulting from reflection of the waves from the opaque object. In this case also an additional path difference can be introduced with the aid of the Wollaston (or Nomarski) prism which in the reflected-light equipment is traversed twice and therefore acts both as an auxiliary and a principal prism (12, 16, 17, 18, 20).

Fig. 4 shows on the left a diagram of a DIC unit for transmitted light using two Wollaston prisms. A body of rectangular cross section is represented as an isotropic, i. e. nonbirefringent object (specimen slide, mounting medium and cover glass are not shown). The condition of the wavefronts at the points a to d in the light path is illustrated in the right-hand part of Fig. 4. The intensity distribution of the DIC image formed in the intermediate image plane, marked e in the diagram, is also discussed. Let the refractive index of the object be smaller than that of the mounting medium: the portions of the wavefronts passing through the object are then accelerated, i. e. they are advanced in relation to the portions of the wavefronts not affected by the object. The resulting wavefront deformation is all the larger, the greater the thickness and smaller the refractive index of the object. In the cases A to C the path difference is assumed to be $+\lambda/2$, and in case D $+\lambda/8$ (diagrams c).

In case A it is assumed that no additional path difference is introduced between Σ_1 and Σ_2 by the principal prism. The function of the principal prism is thus essentially to cancel the angular wave splitting produced by the auxiliary prism. In the process, however, a lateral displacement of the wavefront deformations occurs (d), so that path differences are, after all, introduced between Σ_1 and Σ_2. But the path differences thus caused can only occur at points of the wavefronts where the object has already introduced a change of path difference Γ by the x-coordinate. For the DIC image only the difference of optical paths between Σ_1 and Σ_2 is of importance. Making due allowance for the sign, this is obtained by subtracting the wave Σ_2 from Σ_1[5]. The result is shown in diagram d'. If – following a suggestion by Nomarski (16, 17, 18) – this difference or the differential wave Σ_D is assumed to be an undisturbed reference wave, supplemented by a second, plane wave Σ_0, then the representation in d' is equivalent to d. It is, however, considerably clearer, an advantage that is felt above all with complicated deformed wavefronts.

If *monochromatic* light is used, the simplified relationship $I = I_0 \sin^2(\phi/2)$ holds for the intensity distribution of the DIC image, where I_0 is the maximum intensity in the image and ϕ the phase angle. An angle $\phi = 360°$ corresponds to a path difference $\Gamma = \lambda$. For $\Gamma = -\lambda/2$ corresponding to $\phi = -180°$, $\sin(-180°/2) = -\sin 90° = -1$ and $I = I_0 (-1)^2 = I_0$. The same value is obtained for $\Gamma = +\lambda/2$. For $\Gamma = 0$, I also becomes zero. Thus all values required to indicate the intensity distribution in the x-direction in the diagram e are known. The diagram e' gives an idea of the intensity distribution in the x and y-directions, as in practice the DIC image is seen as a circular disk in the intermediate image plane. In the example, two bright bands can be seen against a completely dark background. These bands indicate that in the corresponding specimen area the optical thickness noticeably differs in the x and/or y-directions from that at directly adjacent points. Only this causes the deformation of the originally plane wavefronts, and only those points in which Γ varies in the x (and/or y-) direction become visible in the DIC image. In the present case, the fringe *spacing* is at the same time a measure of the width of the phase object. The fringe *width* depends on the lateral wave displacement in the equipment; it is chosen so that it is smaller or, at best, identical to the microscopic resolving power. In addition, the fringe width depends on the change of path difference in the x and y-directions (on the gradient of Γ) and thus on the object or the specimen (see examples in Fig. 5).

The DIC image e' in case B of Fig. 4 shows two black fringes on a bright background. Consequently, case B is complementary to A. The inversion of the brightness distribution is brought about by the path difference $+\lambda/2$ between Σ_1 and Σ_2 (diagram d). – In case C (diagram d), Σ_1 lags behind Σ_2 by $\lambda/2$. The same intensity distribution (e') is obtained as in case B. With the principal prism in opposite positions, i. e. symmetrical to the zero position, both these cases can be realized.

In case D, the path difference caused by the object is assumed to be $\lambda/8$ and the path difference introduced by the principal prism $\lambda/4$ (d), contrary to A, B and C. Computation of the intensity distribution yields a different brightness of the two fringes. The impression is that of one-sided oblique illumination of the object (7, 20) with the well-known three-dimensional character[6]. (See also Figs. 48, 81, 443 in Michel [14]).

Fig 5 contains further examples of the formation of DIC images of different isotropic phase objects. Here only those diagrams are included which are essential to the understanding of the problem. The diagrams that have been omitted can easily be added in accordance with the example shown in Fig. 4. If *white* light is used instead of monochromatic light, the contrast of the object is increased by interference colors. This will be explained with the aid of a wavefront (see also [6]), which in a similar form was used already in Fig. 5 (I' d'), to demonstrate the process of image formation by monochromatic light. This is why optical wavelengths and path differences are indi-

[5] This purely formal transformation is carried out exclusively for reasons of convenience and has nothing to do with the subtraction or addition of interfering waves required in interference microscopy. Before reaching the analyzer, Σ_1 and Σ_2 cannot interfere for the simple reason that their vibration directions are mutually perpendicular.

[6] DIC images of a phase object similar to the model under discussion are found elsewhere (20). It should be noted that the photomicrographs published there show **two** parallel furrows in the evaporated film of a specimen slide so that a total of **four** edges can be seen; the model object in Fig. 4 can, of course, produce only two edges. – Case A is, in general, comparable to Fig. 36 a (in 20), case C (and case B) to 36 c, and D corresponds to 36 b.

Fig. 5: Deformed wavefronts with the resulting intensity distribution in the x-direction of the DIC image. Path differences in background = zero (I, II, III) or not zero (I', II', III').

Fig. 6: Color contrast in DIC image.

Fig. 7: Deformation of a plane wavefront by an opaque object with two different phases.

5

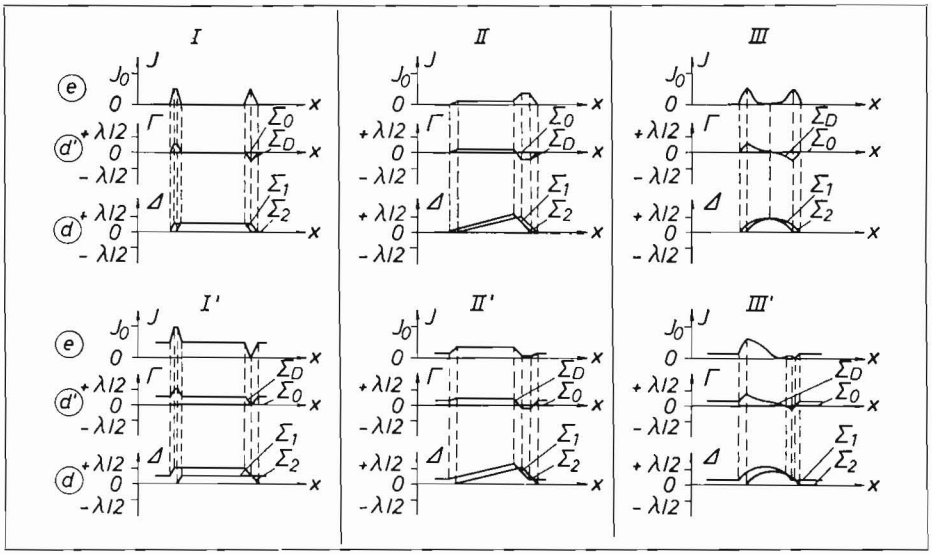

6

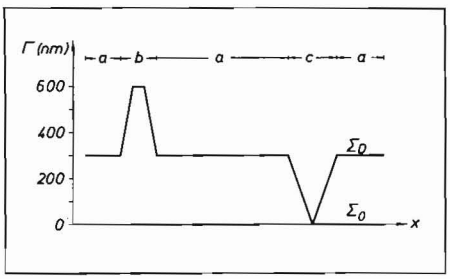

7

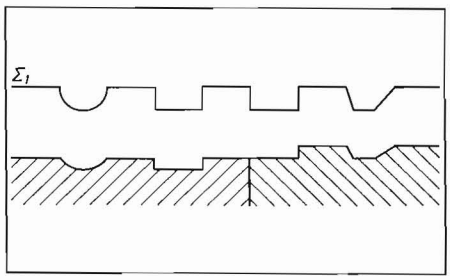

cated on the ordinate in multiples of half the wavelength of the light used. This is, of course, inappropriate in the case of white light.

In the ranges "a" of Fig. 6, Γ is 300 mμ, which according to the Michel-Lévy color chart (19) corresponds to yellow of the first order. In the range b, Γ rises from 300 to 600 mμ, colors ranging from first-order yellow to second-order blue being traversed. However, the intermediate interference colors are less pronounced, since they are relatively crowded due to the considerable variation of Γ. The same applies to the other end in the b range. The color of the plateau (roughly indigo) can, however, be recognized more clearly. In the c range, the variation of Γ with x is not as abrupt as before. The colors are therefore easier to recognize, viz. yellow and first-order white at the upper edges of the furrows, followed by various gray hues which finally become black at $\Gamma = 0$.

The remarks on the formation of the DIC image with transmitted light also hold for reflected light. Characteristic differences exist only in two points. Firstly, a single Wollaston or Nomarski prism represents the auxiliary and principal prisms in the reflected-light equipment. However, such an arrangement can be formally transformed into a transmitted-light setup, as was explained elsewhere (12). Secondly, there is an essential difference in the causes of the wavefronts deformed by the object. In the case of isotropic transparent objects, the local product of refractive index and geometrical thickness of the object determines the form and extent of the wavefront deformation. With opaque objects, the surface relief and thus the geometrical path as well as the phase retardation due to reflection of the wave from the object (21) determine the shape and magnitude of the wavefront deformation (6, 11, 23). This is illustrated by Fig. 7. Let the opaque object consist of two phases (hatched), which impart a different amount of retardation to the reflected waves. A plane wavefront reflected by the object is transformed into the wavefront Σ_1. The rectangular deformations may at the same time serve as an example of ambiguous image formation (see also Fig. 4, B, C; for further examples, see publications 6, 11, 18, 23). Special cases like these are possible in principle if the final image is, among other things, the result of two different magnitudes, such as the thickness and refractive index of the object. An unambiguous interpretation is then possible only on the basis of additional information or measurement using one of these two magnitudes.

References:

[1] *Buchwald, E.:* Einführung in die Kristalloptik, 3rd edition, Sammlung Göschen, Leipzig 1937.

[2] *Flügge, J.:* Leitfaden der geometrischen Optik und des Optikrechnens, Vandenhoeck & Ruprecht, Göttingen 1956.

[3] *Flügge, J.:* Das Phasenkontrastverfahren nach Zernike und Erklärung des Interferenzkontrasts nach Nomarski, lecture given in 1967.

[4] *Françon, M.:* Rev. d'Opt. **31** (1952) 65.

[5] *Françon, M.:* Interférences, Diffraction et Polarisation, Handbuch der Physik XXIV (edited by S. Flügge), Springer-Verlag Berlin-Göttingen-Heidelberg 1956.

[6] *Françon, M.:* Einführung in die neueren Methoden der Lichtmikroskopie, translated by L. Albert, Verlag G. Braun, Karlsruhe 1967.

[7] *Gabler, F.* and *F. Herzog:* Leaflet SD, Interference Contrast, DL D 8/66 by Messrs. C. Reichert, Vienna.

[8] *Gahm, J.:* ZEISS-Information No. 46, pp. 118 – 127.

[9] *Herzog, F.:* Industrie-Anzeiger No. 60 of July 27, 1962.

[10] *Jeglitsch, F.* and *R. Mitsche:* Die Anwendung optischer Kontrastmethoden in der Metallographie, Radex-Rundschau, No. 3/4 (1967), 587 – 596.

[11] *Krug, W., J. Rienitz* and *G. Schultz:* Beiträge zur Interferenzmikroskopie, Akademie-Verlag, Berlin 1961.

[12] *Lang, W.:* Zeiss-Information No. 70 (1968) 113.

[13] *Michel, K.:* Die Grundzüge der Theorie des Mikroskops in elementarer Darstellung. 2nd edition. Wissenschaftliche Verlagsgesellschaft mbH, Stuttgart 1964.

[14] *Michel, K.:* Die Mikrophotographie, 3rd edition, Springer-Verlag, Vienna – New York 1967.

[15] *Mütze, K., L. Foitzik, W. Krug* and *G. Schreiber* (editors): ABC der Optik, Hanau/Main 1961.

[16] *Nomarski, G.:* J. Phys. Radium **16** (1955) 9.

[17] *Nomarski, G.* and *Mme. A. R. Weill:* Bull. Soc. Franc. Minér. crist. **77** (1954) 840.

[18] *Nomarski, G.* and *Mme. A. R. Weill:* Rev. de Métallurgie **52** (1955) 121.

[19] Author not named: Supplement to leaflet S 40-554 of Messrs. Carl Zeiss.

[20] Author not named: Leaflet 41-210 of Messrs. Carl Zeiss.

[21] *Pohl, R. W.:* Optik und Atomphysik, 10th edition, Springer-Verlag, Berlin-Göttingen-Heidelberg 1958.

[22] *Räntsch, K.:* Feinmechanik und Präzision **52** (1944) 75.

[23] *Rienitz, J.:* Mikroskopie **22** (1967) 169.

[24] *Zimmer, H. G.:* Geometrische Optik, Springer-Verlag, Berlin-Heidelberg-New York 1967.